Am J Transl Res 2019;11(3):1569-1580
www.ajtr.org /ISSN:1943-8141/AJTR0085788

Original Article

Alagebrium targets the miR-27b/TSP-1 signaling pathway to rescue Nε-carboxymethyl-lysine-induced endothelial dysfunction

Yihong Chen[1], Wenhao Niu[1], Yu-Chieh Chao[2], Zhiqing He[1], Ru Ding[1], Feng Wu[1], Chun Liang[1]

[1]Department of Cardiology, Shanghai Changzheng Hospital, Second Military Medical University, No. 415, Fengyang Road, Huangpu District, Shanghai 200003, China; [2]Department of Cardiology, Shanghai Renji Hospital, School of Medicine, Shanghai Jiaotong University, No. 1630, Dongfang Road, Pudong New District, Shanghai 200127, China

Received September 20, 2018; Accepted January 21, 2019; Epub March 15, 2019; Published March 30, 2019

Abstract: Nε-carboxymethyl-lysine (CML), a major isoform of advanced glycation end products (AGEs), plays a crucial role in the functional damage of diabetes mellitus. However, it is not clear whether ALT-711 (alagebrium), an inhibitor of AGEs, is capable to rescue CML-induced poor angiogenesis, as well as the underlying mechanism. MicroRNA-27b (miR-27b) promotes angiogenesis through down-regulation of anti-angiogenic protein thrombospondin-1 (TSP-1). Here, we used diabetic mice with hindlimb ischemia to investigate whether miR-27b/TSP-1 signaling is involved in the pathology of critical limb ischemia (CLI) in diabetes mellitus. We additionally examined the effect of ALT-711 on the tube formation of endothelial cells treated with CML-BSA. Compared with control group, the lower blood flow recovery was observed in the ischemic lower limbs of diabetic mice, with decreased expression of vascular endothelial growth factor (VEGF) and miR-27b and increased TSP-1 expression. CML-BSA reduced the tube formation ability of endothelial cells, decreased VEGF and miR-27b expression, and increased TSP-1 expression, whereas this trend was reversed by ALT-711. The miR-27b mimic promoted tube formation, increased VEGF expression, and decreased TSP-1 expression, whereas these effects were abolished by TSP-1 overexpression. Moreover, miR-27b silencing suppressed ALT-711-induced promotion of tube formation under CML-BSA treatment, with reduced VEGF and augmented TSP-1 expression. Taken together, the present study demonstrated that ALT-711 can rescue CML-induced functional angiogenesis damage via miR-27b/TSP-1 signaling cascades. These results indicate new therapeutic strategies for diabetes patients with CLI.

Keywords: Nε-carboxymethyl-lysine, alagebrium, miR-27b, TSP-1, HUVECs, critical limb ischemia

Introduction

Patients with peripheral artery disease (PAD) experience an elevated risk of lower limb ischemia because of narrowed or occluded arteries with decreased blood flow. It is estimated that more than 200 million people are diagnosed with PAD worldwide [1]. It's reported that 10%-25% of people will eventually suffer from PAD among individuals aged ≥ 55 years; however, this number increases to about 40% in people aged > 80 years [2, 3]. Among the risk factors, diabetes mellitus is considered as a vital risk factor for PAD [4]. Furthermore, patients with PAD and diabetes have an augmented risk of critical limb ischemia (CLI), the most severe PAD outcome [5]. And the neovascularization disorder induced by hyperglycemia account for the main reason for the increased risk of CLI [6-8]. However, the molecular mechanisms associating diabetes with CLI remains not fully clarified.

Advanced glycation end products (AGEs) are protein or lipid modifications that are widely distributed in the diabetic vasculature and trigger the initiation of multiple-organ damage in the diabetic microenvironment [9]. And hyperglycemia can promote the vessel wall accumulation of AGEs and thereby lead to high vessel permeability through destroying the cell-cell junctions of endothelium and inducing endothe-

lial cell death [10, 11], suggesting that AGE might play a vital role in the pathogenesis of PAD. Nε-carboxymethyl-lysine (CML), a major immunogen and isoform of AGEs in plasma and tissue proteins, is associated with cardiovascular mortality [12]. Recently, Liu et al. [13] found that the AGEs inhibitor alagebrium (ALT-711; 3-phenacyl-4, 5-dimethylthiazolium chloride) has been shown to improve vessel resistance and cardiovascular function impaired by diabetes via the breakage of AGE-related collagen cross-linking. However, the effects and mechanisms of ALT-711 on CML-induced angiogenesis damage need to be further explored.

MicroRNAs (miRNAs) are small, non-coding RNA molecules that repress gene expression by binding to the 3'UTR of their target messenger RNAs (mRNAs) [14-16]. miRNAs play important roles in the physiological pathway of CLI [17-19]. For instance, miR-27b is expressed at low levels in diabetes patients and mice models, and up-regulation of miR-27b has been shown to enhance proliferation, adhesion, and tube formation, and inhibit the apoptosis of bone marrow-derived angiogenic cells through down-regulation of anti-angiogenic thrombospondin-1 (TSP-1), an extracellular glycoprotein that modulates cell-cell interactions [20, 21]. Besides, overexpression of miR-27b enhanced platelet angiogenic activities by reducing TSP-1 protein expression [22]. Together, these findings indicate that miR-27b/TSP-1 signaling plays a crucial role in maintaining angiogenic ability.

The aim of the present study is to determine whether and how ALT-711 improves CML-induced angiogenic function damage. We postulate that miR-27b/TSP-1 signaling is a promising target for ALT-711 therapy against CML damage. We evaluated the expression of miR-27b and TSP-1 in ischemic hindlimbs of diabetes mice and control mice (non-diabetic mice). We then used the commercial products CML-BSA and ALT-711, in combination with the miR-27b mimic/inhibitor and TSP-1 overexpression plasmids, to determine the effects of ALT-711 and miR-27b/TSP-1 on angiogenesis *in vitro*. These results help expand our understanding of diabetes with CLI and represent a promising therapeutic strategy for clinical settings.

Materials and methods

Animals

Male BALB/c mice, 4-6-week old, were purchased from the Institute of Laboratory Animal Science CAMS & PUMC (Beijing, China). The mice were divided into control and diabetes groups, with eight mice in each group. Animals were kept on a 12-hour light/dark cycle with food and water available ad libitum in the Animal Center of Second Military Medical University. All efforts (such as pain relief during the experiments and natural housing) were made to relieve the suffering of mice and all procedures were performed in accordance with the National Institutes of Health Guidelines for the Care and Use of Laboratory Animals.

Diabetic mice with hindlimb ischemia induction

Diabetic mouse models were induced through intraperitoneal streptozotocin (Sigma-Aldrich, MO, USA) injection [23]. In detail, mice were injected with citrate buffer (4.92 mol/ml sodium citrate, pH 4.2-4.5; n = 8) or streptozotocin (50 mg/kg; n = 8) dissolved in sterile citrate buffer for 5 consecutive days. Blood glucose levels were measured 7, 14, and 21 days after injection. Blood glucose levels > 12.0 mmol/L indicated successful induction of type 1 diabetes mouse models and these mice were selected for further experiments.

Three weeks after streptozotocin injection, hindlimb ischemia was induced in mice of each group by left hindlimb artery devascularization. Mice aged 7-9 weeks were anesthetized by intraperitoneal injection of 2% pentobarbital sodium (50 mg/kg). During the operation, the spin iliac artery, femoral profound artery, the branch of the femoral artery, and the knee joint were ligated and excised to form hindlimb ischemia. The right femoral artery was exposed but not dissected as the non-ischemic control.

Laser Doppler perfusion imaging (LDPI)

LDPI (Perimed Instruments AB, Stockholm, Sweden) was conducted on mice immediately, 2 weeks, 4 weeks and 6 weeks after ischemic surgery to assess the blood flow recovery ratio in ischemic hindlimbs. Blood flow recovery ratio = Ischemic limb perfusion (left hindlimb)/Non-

ischemic limb perfusion (right hindlimb) × 100%. Colored histogram pixels indicated the blood reperfusion of ischemic and non-ischemic limbs.

Histopathology analysis and immunohistochemical staining

Six weeks after ischemic surgery, mice were sacrificed by an overdose of isoflurane and the hindlimbs were harvested and stored in liquid nitrogen for further research. For histopathologic analysis, tissues were fixed with formalin and embedded with paraffin, and cut into 6-μm-thick sections. The diameter of the intermuscular artery lumen was evaluated by hematoxylin & eosin (HE) staining, as in a previous report [24]. Immunohistochemical staining was performed to detect CD31 (Cell Signaling Technology, CA, USA) expression as described previously [25].

X-ray angiography

X-ray angiography was performed proximal to the branch point of the common iliac arteries along with injection of contrast medium (barium sulfate, 0.5 g/ml) in mice after 6 weeks of ischemic surgery. Angiography was assessed with an angiographic system (MX-20, Faxitron, USA). The length, number, and vessel area of the hypogastric artery and all whole, visible, collateral branches were measured using Image J software.

Cell culture and treatment

Human umbilical cord-derived endothelial cells (HUVECs) were purchased from American Type Culture Collection (ATCC, VA, USA) and cultured in Vascular Cell Basic Medium plus Endothelial Cell Growth Kit-VEGF (ATCC, VA, USA). Cells were maintained in a humidified incubator at 37°C in an atmosphere with 5% CO_2.

HUVECs were incubated with 7.5, 15, 30, 60, or 120 mg/mL CML-BSA (No. STA-314, Cell-Biolabs, CA, USA) for 24 h. AGEs inhibitor ALT-711 (20 μg/mL; MedChemExpress, China) was added to cell culture medium for 24 h with isopycnic DMSO used as the negative control.

Cell transfection

The human *TSP-1* over-expression plasmid (OE-TSP-1) and the corresponding negative control (OE-NC) were purchased from OriGene (CA, USA). The miR-27b mimic/inhibitor, and their negative control sequences, were synthesized by GenePharma (Shanghai, China). For cell transfection, HUVECs were transfected with OE-TSP-1, -miR-27b-mimic or inhibitor-miR-27b using Lipofectamine 2000 (Invitrogen, CA, USA), following the manufacturer's instructions.

Western blotting analysis

Proteins were extracted from tissue samples and cells with RIPA buffer (Invitrogen, CA, USA) and quantified using the BCA Protein Assay Kit (Thermo Fisher Scientific, MA, USA). Then, equal amounts of protein (20-30 mgg) were separated by 10% SDS-PAGE and transferred to PVDF membranes (Millipore, Billerica, MA, USA). Then, the membranes were blocked with 5% non-fat milk and incubated with primary antibodies against VEGF (Cell Signaling Technology, CA, USA), GAPDH (Thermo Fisher Scientific, MA, USA), and TSP-1 (Cell Signaling Technology, CA, USA), followed by incubation with the corresponding secondary antibodies (ZSGB-BIO, Beijing, China). After the membranes being washed three times with phosphate-buffered saline containing Tween 20, the proteins were enhanced by ECL reagent (Millipore, MA, USA) and detected on a ChemiDoc Touch system (Bio-Rad, IQ, USA).

Quantitative real time PCR (qRT-PCR)

Total RNA and miRNA were isolated with Trizol reagent (Invitrogen, CA, USA) and the miRNeasy Mini Kit (Qiagen, Valencia, CA), respectively. cDNA synthesis was performed using the miScript II RT kit (Qiagen, Valencia, CA), followed by qRT-PCR using the miScript SYBR Green PCR kit (Qiagen, Valencia, CA). miRNA expression was detected by primer from miScript Primer Assays (Qiagen, Valencia, CA) and normalized to U6 level. Other specific primers, designed for qRT-PCR analysis, are listed:

(Human) TSP-1-forward: 5'-TCAGGAAATACTGCCTGTAGAGT-3', (Human) TSP-1-reverse: 5'-AGCCAGTAGAGAACAAATAAGCA-3'; (Mouse) TSP-1-forward: 5'-ACTGGTGAAGGGCCAAGATCT-3', (Mouse) TSP-1-reverse: 5'-GGATCAGGTTGGCATTCTCAA-3'; (Human) VEGF-forward: 5'-AAAGCGCAAGAAATCCCGTC-3', (Human) VEGF-reverse: 5'-GGTGAGAGATCTGGTTCCCG-3'; (Mouse) VEGF-forward: 5'-CACAGCAGATGTGAATGCAG-3', (Mouse) VEGF-reverse: 5'-TTTACACGTCTGCGGATCTT-3'; (Human) GAPDH-forward: 5'-TG-

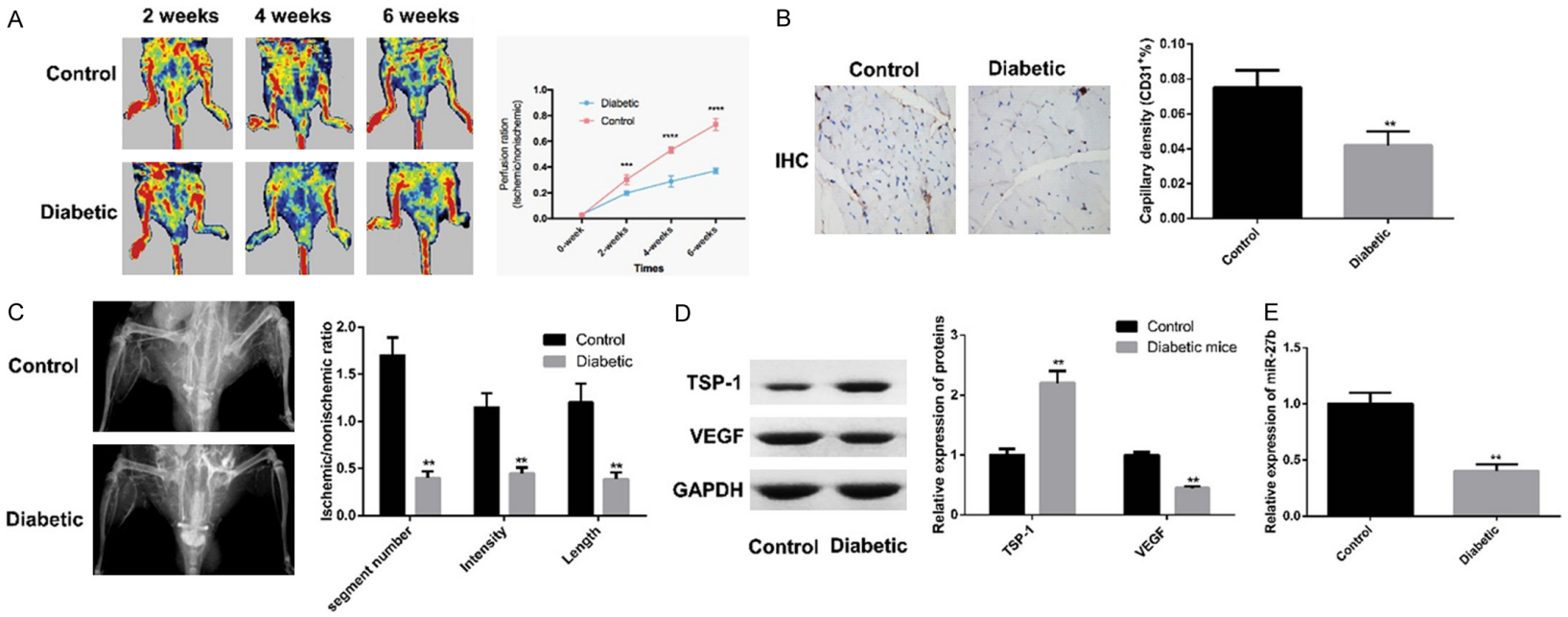

Figure 1. Decreased miR-27b is involved in impaired angiogenesis in diabetes mellitus. A. Representative images of perfusion recovery in ischemic hindlimbs from each group 2, 4 and 6 weeks after operation and quantitative evaluation by Laser Doppler perfusion imaging. B. Representative image of CD31 immunohistochemistry in ischemic hindlimbs to assess capillary density in each group. C. Representative images of angiography in ischemic hindlimbs taken by X-ray 6 weeks post-operation. The microangiography of each group was measured by segment number, total length, and vessel area in the limited zone. D. VEGF and TSP-1 protein expression in ischemic hindlimbs from control and diabetic mice are detected by western blotting analysis. E. miR-27b expression in ischemic hindlimbs from normal and diabetic mice are determined by qRT-PCR. (Scale bar = 200 mm; n = 8 per group; $^{**}P < 0.01$, $^{***}P < 0.001$, $^{****}P < 0.0001$).

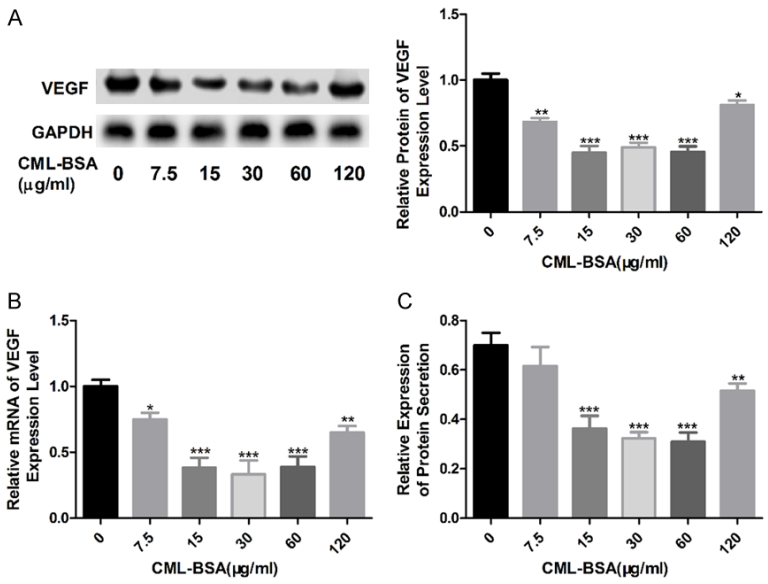

Figure 2. CML-BSA stimulation suppresses VEGF expression in HUVECs. A. Western blotting analysis of the protein level of VEGF after HUVECs were treated with 0, 7.5, 15, 30, 60 or 120 μg/mL CML-BSA for 24 h. B. The mRNA level of VEGF are determined by qPCR after HUVECs were treated with 0, 7.5, 15, 30, 60 or 120 μg/mL CML-BSA for 24 h. C. ELISA assay is used to detected the secreted VEGF protein level in HUVECs treated with 0, 7.5, 15, 30, 60 or 120 μg/mL CML-BSA for 24 h. (n = 3, $^{*}P < 0.05$, $^{**}P < 0.01$, $^{***}P < 0.001$).

AAGACGGGCGGAGAGAAAC-3', (Human) GAPDH-reverse: 5'-TGATGACAAGCTTCCCGTTCT-3'; (Mouse) GAPDH-forward: 5'-TCACCACCATGGAGAAGGC-3', (Mouse) GAPDH-reverse: 5'-GCTAAGCAGTTGGTGGTGCA-3'.

Tube formation assay

The tube formation assay was performed as described previously [26]. In brief, each well of a 96-well plate was coated with 50 μL Matrigel matrix (BD, Bedford, MA, USA), then HUVECs were seeded on the pre-coated wells at a density of 1×10^4 cells/well. After 24-h incubation, images of tube morphology were recorded using an inverted microscope (Olympus IX51; Olympus, Inc.) at × 40 magnification and tube lengths were measured in six random fields per well.

Enzyme-linked immunosorbent assay (ELISA)

HUVEC supernatant was collected 3 days after incubation with CML-BSA or ALT-711 treatments for 24 h to measure secreted VEGF. Secreted VEGF protein was quantified with human ELISA kits (Thermo Fisher Scientific, MA, USA) based on the manufacturer's instructions.

Statistical analyses

All results are expressed as means ± standard deviation (SD). Data were analyzed with GraphPad Prism 6.0 software, using Student's unpaired *t* test to assess differences between two groups or one-way ANOVA with Bonferroni correction for multiple group comparison. Differences were considered significant at $P < 0.05$.

Results

Decreased miR-27b was involved in impaired angiogenesis in diabetes mellitus

To investigate the function of miR-27b in angiogenesis in diabetes mellitus, we constructed a diabetic mouse model with hindlimb ischemia. Compared with the control group, in which mice only underwent induction of hindlimb ischemia, the blood flow recovery of ischemic lower extremities was obviously decreased in mice in diabetic group (**Figure 1A**). Besides, the immunohistochemical staining intensity of CD31, which was used to evaluate capillary density was decreased in the ischemic hindlimbs of the diabetic group (**Figure 1B**). And the angiography results revealed a similar trend; these were analyzed by three different criteria: segment number, intensity, and total length (**Figure 1C**). In addition, we detected the expression of angiogenic mediator proteins, VEGF and TSP-1, in the tissue of ischemic legs of the two groups. And results showed that VEGF protein expression decreased and TSP-1 protein expression increased in mice hindlimb tissues of diabetic group (**Figure 1D**). And the expression of miR-27b was significantly lower in the diabetic group than that in the control group. (**Figure 1E**). These results suggest that diabetes aggravates hindlimb ischemic damage and hampers angiogenesis, in which miR-27b might play an important role.

CML-BSA stimulation suppressed VEGF expression in HUVECs

To explore the influence of diabetes on angiogenesis *in vitro*, we used different concentra-

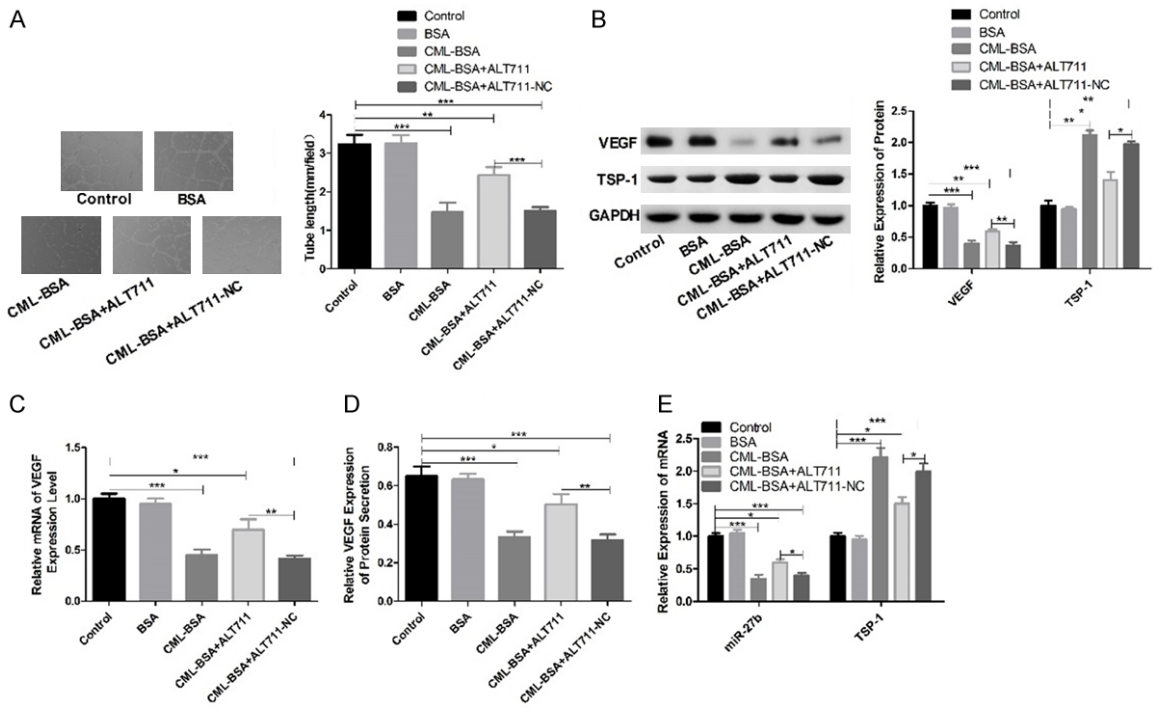

Figure 3. AGEs inhibition rescued the angiogenic function of HUVECs treated with CML-BSA and increased miR-27 expression. A. HUVEC tube formation in untreated cells and cells treated with BSA, CML-BSA (30 μg/mL), CML-BSA + DMSO, and CML-BSA + ALT-711 (20 μg/mL) for 24 h. Tube network assays from each treatment group show that CML-BSA suppresses the angiogenesis of HUVECs, and that reduced tube formation is rescued by ALT-711. Representative images are shown on the left. B, C. VEGF/TSP-1 protein and mRNA expression in HUVECs from each group are detected by western blotting and qRT-PCR assays, respectively. D. Secreted VEGF protein expression from HUVECs of each group is assessed by ELISA. E. qRT-PCR was performed to assess miR-27 and *TSP-1* expression in HUVECs with different treatments as indicated. (n = 3, $^{*}P < 0.05$, $^{**}P < 0.01$, $^{***}P < 0.001$).

tions of CML-BSA, a mimic of diabetic damage to stimulate HUVECs. Following CML-BSA stimulation of HUVECs, VEGF expression was measured. Western blotting and qRT-PCR analyses showed that VEGF protein and mRNA expression were suppressed in HUVECs treated with various concentrations of CML-BSA (**Figure 2A**, **2B**). A similar pattern was revealed by ELISA analysis of HUVEC-secreted VEGF protein expression (**Figure 2C**). And the decrease of secreted VEGF protein expression was most pronounced in the 30 μg/mL CML-BSA group, hence, we chose the 30 μg/mL of CML-BSA for further analyses.

Inhibitor of AGEs (ALT-711) rescued the angiogenic function of HUVECs treated with CML-BSA and increased miR-27 expression

We next assessed whether the ALT-711 AGEs inhibitor could rescue CML-BSA-induced angiogenic function damage and examined its possible mechanism *in vitro*. Compared with cells in control or BSA group (CML-BSA negative control), HUVECs treated with CML-BSA displayed distinctly impaired tube formation (**Figure 3A**) and reduced VEGF protein, secreted protein, and mRNA expressions (**Figure 3B-D**), as well as increased TSP-1 expression (**Figure 3B**). In contrast, ALT-711 rescued the CML-BSA-induced impaired angiogenesis (**Figure 3A**), and upregulated VEGF protein, mRNA, and secreted protein expressions and decreased TSP-1 expression (**Figure 3B-D**). Furthermore, qRT-PCR analysis suggested that CML-BSA treatment significantly decreased miR-27b expression and increased TSP-1 expression, and this expression trend was partially reversed by ALT-711 in HUVECs (**Figure 3E**). These findings indicate that the AGEs inhibitor promotes the angiogenesis of endothelial cells through up-regulating the expression of miR-27b.

miR-27b improved HUVEC angiogenesis via negative regulation of TSP-1

To reveal the effect of miR-27b on HUVEC angiogenesis and its downstream molecular path-

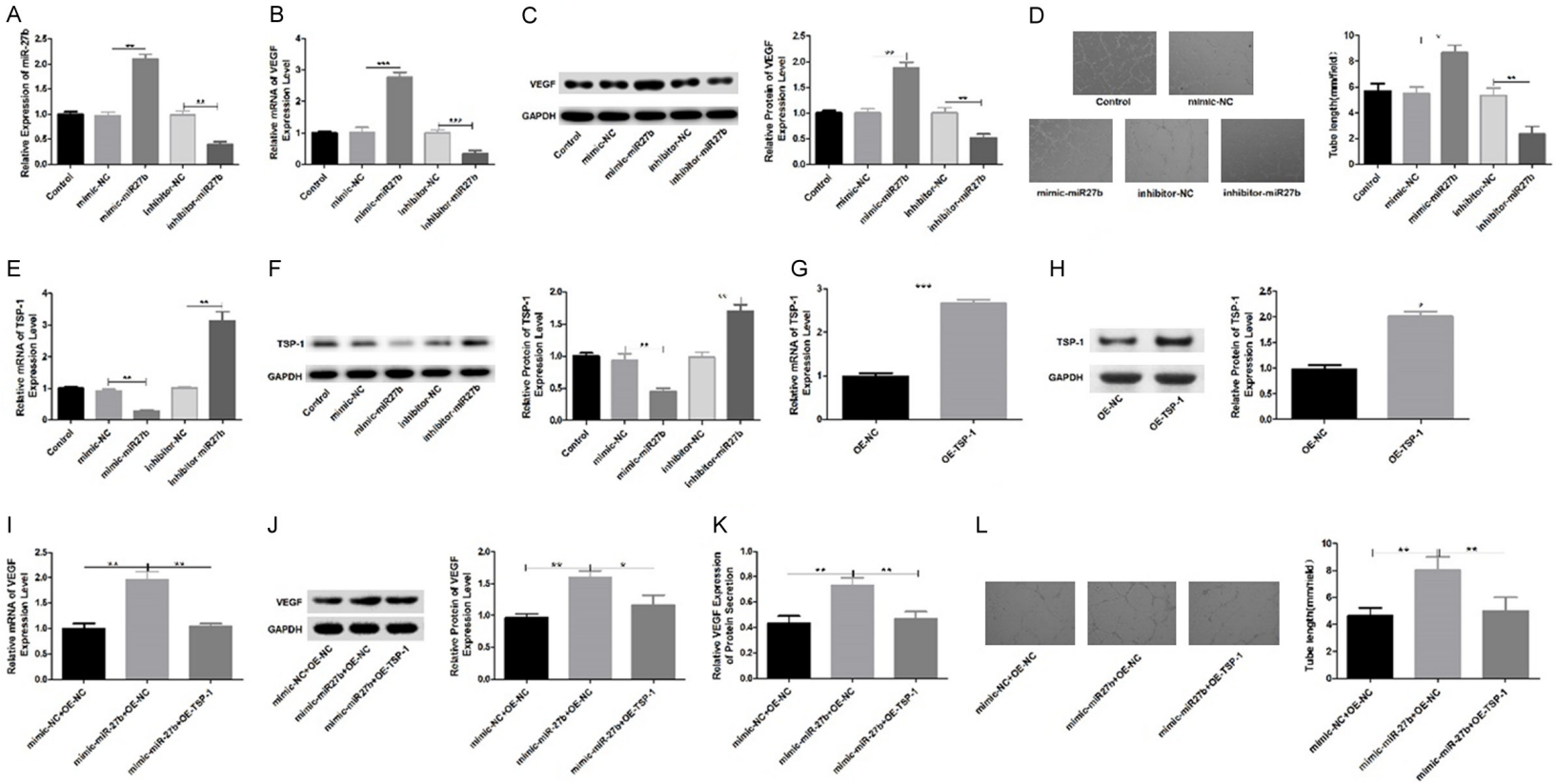

Figure 4. miR-27b improves angiogenesis in HUVECs by negatively regulating TSP-1. A. qRT-PCR is used to determine miR-27b expression in HUVECs transfected with miR-27b mimic/inhibitor and the relevant control. B, C. *VEGF* mRNA and protein expression in miR-27b mimic/inhibitor transfected HUVECs are detected by western blotting and qRT-PCR assays, respectively. D. Tube formation assay is performed to assess the tube formation ability of HUVECs transfected with miR-27b mimic/inhibitor. Representative images are shown on the left. E, F. Decreased TSP-1 protein expression in HUVECs transfected with miR-27b mimic, and increased TSP-1 protein expression in HUVECs transfected with miR-27b inhibitor, which is detected by qRT-PCR and western blotting. G, H. qRT-PCR and western blotting assays are used to measure the mRNA and protein expressions of TSP-1 in HUVECs transfected with OE-TSP-1 and OE-NC. I, J. mRNA and protein expression of VEGF in HUVECs transfected with mimic-miR-27b and OE-TSP-1 are detected by qRT-PCR and western blotting assays. K. Secreted VEGF protein from HUVECs transfected with miR-27b mimic and OE-TSP-1 are assessed by ELISA. L. Tube formation assay demonstrating that the effect of miR-27b mimic on angiogenesis in HUVECs was suppressed by OE-TSP-1. Representative images are on the left. (n = 3, $^{*}P < 0.05$, $^{**}P < 0.01$, $^{***}P < 0.001$).

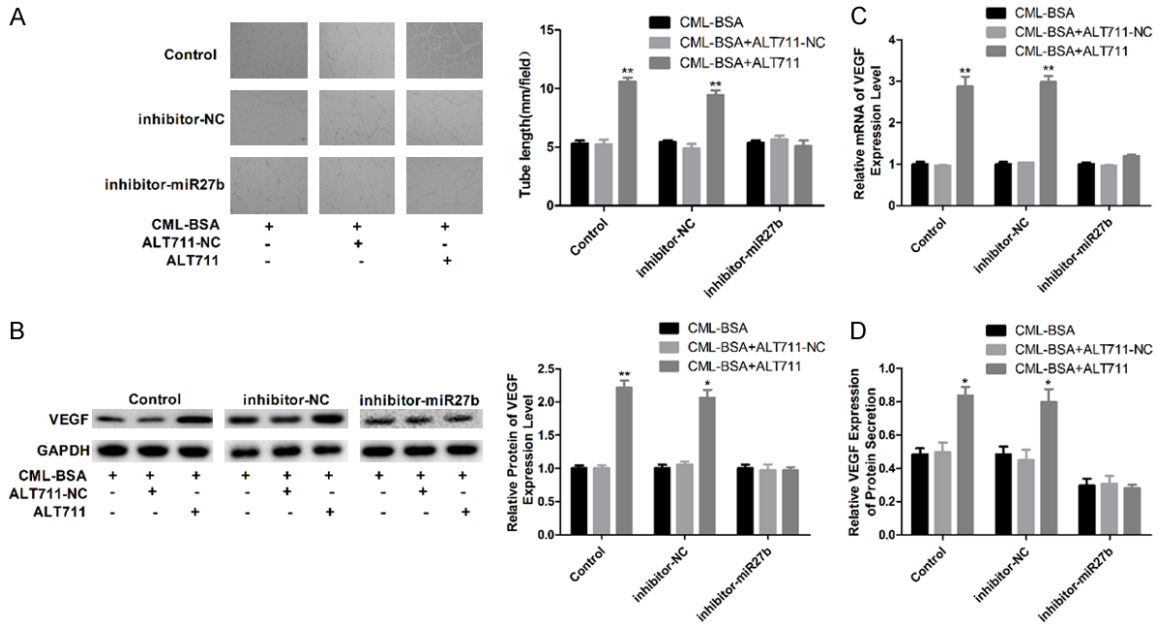

Figure 5. ALT-711 targets miR-27b to ameliorate CML-BSA-mediated angiogenesis impairment. A. Tube formation in HUVECs transfected with miR-27 inhibitor and treated with CML-BSA or CML-BSA plus ALT-711/ALT-711-NC. Representative images are on the left. B, C. Western blotting and qRT-PCR assay are used to detect VEGF expression in protein and mRNA levels and results showed that CML-BSA treatment resulted in decreased VEGF protein and mRNA expression in HUVECS when ALT-711 function was hampered by miR-27 inhibitor. D. ELISA assay analysis of the secreted VEGF protein levels in HUVECs of each group. (n = 3, $^{*}P < 0.05$, $^{**}P < 0.01$).

ways, we recruited miR-27b mimic/inhibitor to up/downregulate miR-27b expression in HUVECs. The transfected efficiency of miR-27b mimic/inhibitor was confirmed by qRT-PCR (**Figure 4A**). Up-regulation of miR-27b enhanced VEGF expression in protein and mRNA levels in HUVECs (**Figure 4B**, **4C**). Importantly, up-regulation of miR-27b significantly improved HUVEC tube formation (**Figure 4D**). Besides, miR-27b mimic suppressed TSP-1 protein expression in HUVECs, and miR-27b inhibitor markedly up-regulated TSP-1 expression in protein and mRNA levels (**Figure 4E**, **4F**). We next explored if TSP-1 involves in angiogenesis inhibition induced by miR-27b. A significant increase in TSP-1 expression in HUVECs was observed following OE-TSP-1 transfection (**Figure 4G**, **4H**). VEGF protein and mRNA expression were elevated in HUVECs transfected with the miR-27b mimic, and partially reversed upon TSP-1 overexpression in combination with the miR-27b mimic. This effect was also observed when measuring VEGF secreted protein expression (**Figure 4I-K**). TSP-1 overexpression delayed the enhanced tube formation ability regulated by the miR-27b mimic (**Figure 4L**). These data confirm that the miR-27b facilitates the angiogenesis of HUVECs via negative regulation of TSP-1 expression.

ALT-711 targeted miR-27b/TSP-1 pathway to ameliorate impaired angiogenesis induced by CML-BSA

Then, we assessed whether ALT-711 is capable to rescue CML-BSA-induced HUVEC dysfunction through modulation of miR-27b/TSP-1 signaling *in vitro*. The addition of ALT-711 to CML-BSA-treated HUVECs enhanced tube formation; this effect was suppressed by miR-27b inhibitor transfection (**Figure 5A**). Western blot and qRT-PCR results showed that increased VEGF expression induced by ALT-711 under CML-BSA treatment was reduced when miR-27b was silenced with miR-27b inhibitor transfection (**Figure 5B**, **5C**), as well as VEGF secreted protein level (**Figure 5D**). However, following ALT-711 treatment, TSP-1 protein levels and mRNA expression decreased (**Figure 6A**, **6B**), which rescued the impaired angiogenic function of HUVECs under CML-BSA stimulation. And the effect of ALT-711 on TSP-1 expression was reversed when miR-27b was silenced in HUVECs treated with CML-BSA (**Figure 6A**, **6B**).

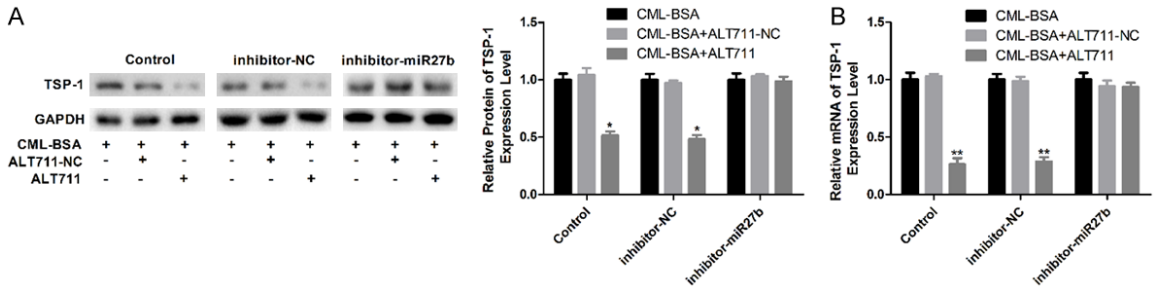

Figure 6. TSP-1 modulation via miR-27b contributes to the effect of ALT-711 on CML-BSA-mediated dysfunction of HUVECs. A. Western blotting analysis of TSP-1 protein expression, and results showed that TSP-1 expression in HUVECs treated with ALT-711 under CML-BSA condition is enhanced by miR-27b inhibitor. B. qRT-PCR analysis of *TSP-1* mRNA expression in HUVECs transfected with miR-27b inhibitor/NC in response to treatment with CML-BCA or CML-BSA plus ALT-711/ALT-711-NC. (n = 3, $^{*}P < 0.01$, $^{**}P < 0.001$).

Together, these results show that ALT-711 ameliorates the impaired angiogenesis in CML-BSA-treated HUVECs by regulating miR-27b/TSP-1 signaling.

Discussion

CLI has been shown to occur in 11% of PAD patients, while it increases to 20% in patients aged > 70 years [27]. The prognosis for patients with CLI is extremely poor with only 25-40% patients have the change to accept lower limb amputation and 20% patients survival [28]. Therapeutic angiogenesis is a potential approach to stimulate neovascularization in extreme damaged tissue to improve limb perfusion and tissue regeneration [29]. However, AGEs produced by long-term hyperglycemia is identified as a main reason to cause tissue injury and neovascularization damage [30, 31], which may partly explain the high prevalence of CLI in diabetes patients. In this study, we observed that blood flow recovery and diameter of the intermuscular artery lumen were decreased in mice in the diabetic group (Supplementary Figure 1), as well as the decreased expression of CD31, a endothelial cell marker, and the reduced lateral branch circulation capacity in ischemic hindlimbs, suggesting that the pathologic niche of diabetes might contribute to angiogenesis dysfunction. Therefore, it's worthy to explore the mechanism underlying AGE in exacerbation of CLI, hoping to find effective therapies for CLI combined with diabetes mellitus. And the present study make clear that CML-BSA impairs the angiogenesis of ECs through interaction with miR-27b/TSP-1 signaling molecules.

ALT-711, an AGEs inhibitor, was first used to analyze CML-BSA-induced angiogenesis dysfunction. In diabetic ApoE-/- mice, ALT-711 alleviates glomerular fibrogenesis and inflammation though RAGE activation [32] and significantly improves heart mechanical and major vascular resistance [33]. However, the effect of ALT-711 against the damage induced by CML-BSA in HUVECs had not been examined. We proposed the hypothesis that ALT-711 rescued angiogenesis dysfunction induced by CML-BSA. To the best of our knowledge, our results demonstrate, for the first time, that CML-BSA decreased VEGF expression and secretion in HUVECs in a dose-independent manner, which could be partially reversed by ALT-711.

Angiogenesis involves the stimulation, formation, and stabilization of new blood vessels, and VEGF plays a role as "master switch" during these processes. Consistently with previously reported results [34], the delay of VEGF protein expression correlated with the poor neovascularization of diabetic mice. In contrast, levels of TSP-1, a 142-KDa glycoprotein that functions as an endogenous protein inhibitor of angiogenesis [35], were drastically enhanced. High glucose levels have been confirmed to be a cell-type-specific regulating factor of TSP-1 in post-transcription level [36]. For example, pancreatic islets treated with 16.7 mmol/L glucose showed a significant decrease in VEGF expression and increase in TSP-1 expression as compared cells treated with 5.5 mmol/L glucose; besides, high glucose inhibited the angiogenesis of human umbilical vein endothelial cells (HUVECs) [37]. Additionally, the TSP-1-CD47 axis has been shown to regu-

late angiogenesis through inhibition of VEGF-Akt-eNOS [38]. All findings illustrate that high glucose damage the angiogenesis of cells through regulating TSP-1 and VEGF expression. Consistently, we observed that the expression of VEGF was decreased in the ischemic lower limb tissues from diabetic mice as compared with the normal mice, as well as increased TSP-1 expression.

MicroRNAs, which are single-stranded small non-coding RNAs that induce mRNA degradation or repress translation, are dysregulated in multiple of diseases, including tumors and atherosclerosis [39, 40]. Several results suggest that miR-27b has a pro-angiogenic function. For instance, Biyashev et al. [41] reported that miR-27b inhibition severely impairs vessel sprouting and filopodia formation in zebrafish and mouse tissues by inhibiting Delta-like ligand 4 and Sprouty-2. Our results show that miR-27b is also suppressed in diabetic mice with limb ischemia. Besides, miR-27b was suppressed in HUVECs damaged by CML-BSA and elevated after using ALT-711 against CML-BSA, while no major differences were observed for other miRNAs (Supplementary Figure 2). An opposite trend was observed for *TSP-1* mRNA expression. To reveal the interaction between miR-27b and TSP-1 in HUVECs, we transfected HUVECs with miR-27b mimic/inhibitor and OE-TSP-1 plasmids. Up-regulation of miR-27b clearly promoted the tube formation of HUVECs, increased VEGF expression, and attenuated *TSP-1* mRNA expression, whereas these results were all blocked by TSP-1 over-expression, suggesting that miR-27b promotes the angiogenesis through negatively regulating *TSP-1* expression. Our data are consistent with those previously reported, in that miR-27b promotes angiogenesis via down-regulating TSP-1 expression in diabetic mice [21, 22].

Collectively, the present study provides meaningful clues about the role of ALT-711/miR-27b/TSP-1 signaling pathway in protecting epithelial cells from AGE-mediated dysfunction; however, several gaps in our knowledge still need to be filled. The functional improvement conferred by ALT-711 in diabetic animals with CLI needs to be confirmed by further research in a more complex *in vivo* environment. Additionally, although it has been described previously [21], we did not employ a luciferase target assay to directly assess the relationship between miR-27b and TSP-1. Moreover, the nature of the TSP-1 and VEGF interaction needs to be examined and defined. Further, it should be noted that the CML-BSA doses used in this investigation were higher than those reported in other studies. In patients with chronic kidney disease, the maximum concentration of CML used is 18.5 mg/L [43], and no observable impairment of migration, apoptosis, or tube formation was observed in endothelial progenitor cells after treatment with 250-1000 μg/ml CML [42]. Therefore, it is worth exploring the pathological mechanism of AGEs using a broader concentration range.

In conclusion, our results demonstrate that ALT-711, an AGEs inhibitor, rescues CML-induced angiogenesis dysfunction via modulation of miR-27b/TSP-1 pathway, which may be useful for the development of improved therapeutic intervention for patients with diabetes mellitus and CLI.

Acknowledgements

This work was supported by grants from the National Natural Science Foundation of China (grant no. 91539118, 81611130092, 3117-1130, 81270405, 30971101, to C. Liang; grant no. 81503371, to F. Wu; grant no. 81400336, to R. Ding), the Shanghai Municipal Natural Science Foundation 13ZR1413600 (to R. Ding) and 15401931500 (to Z.Q. He). Dr Y.H.Chen was awardee of China Scholarship Council 201703170134. Also, we would like to thank Editage [www.editage.cn] for English language editing.

Disclosure of conflict of interest

None.

Address correspondence to: Drs. Chun Liang and Feng Wu, Department of Cardiology, Shanghai Changzheng Hospital, Second Military Medical University, Floor 26, No. 415, Fengyang Road, Huangpu District, Shanghai 200003, China. Tel: +86-021-81885291; Fax: +86-021-63520020; E-mail: chunliang@smmu.edu.cn (CL); wufengmed1988@outlook.com (FW)

References

[1] Fowkes FG, Rudan D, Rudan I, Aboyans V, Denenberg JO, McDermott MM, Norman PE, Sampson UK, Williams LJ, Mensah GA and

Criqui MH. Comparison of global estimates of prevalence and risk factors for peripheral artery disease in 2000 and 2010: a systematic review and analysis. Lancet 2013; 382: 1329-1340.
[2] Norman PE, Eikelboom JW and Hankey GJ. Peripheral arterial disease: prognostic significance and prevention of atherothrombotic complications. Med J Aust 2004; 181: 150-154.
[3] Bergiers S, Vaes B and Degryse J. To screen or not to screen for peripheral arterial disease in subjects aged 80 and over in primary health care: a cross-sectional analysis from the BELFRAIL study. BMC Fam Pract 2011; 12: 39.
[4] Tapp RJ, Balkau B, Shaw JE, Valensi P, Cailleau M and Eschwege E. Association of glucose metabolism, smoking and cardiovascular risk factors with incident peripheral arterial disease: the DESIR study. Atherosclerosis 2007; 190: 84-89.
[5] Adler AI, Stevens RJ, Neil A, Stratton IM, Boulton AJ and Holman RR. UKPDS 59: hyperglycemia and other potentially modifiable risk factors for peripheral vascular disease in type 2 diabetes. Diabetes Care 2002; 25: 894-899.
[6] Jude EB, Oyibo SO, Chalmers N and Boulton AJ. Peripheral arterial disease in diabetic and nondiabetic patients: a comparison of severity and outcome. Diabetes Care 2001; 24: 1433-1437.
[7] Criqui MH and Aboyans V. Epidemiology of peripheral artery disease. Circ Res 2015; 116: 1509-1526.
[8] Espinola-Klein C and Savvidis S. Peripheral arterial disease: epidemiology, symptoms and diagnosis. Internist (Berl) 2009; 50: 919-926.
[9] Goldin A, Beckman JA, Schmidt AM and Creager MA. Advanced glycation end products: sparking the development of diabetic vascular injury. Circulation 2006; 114: 597-605.
[10] Semba RD, Nicklett EJ and Ferrucci L. Does accumulation of advanced glycation end products contribute to the aging phenotype? J Gerontol A Biol Sci Med Sci 2010; 65: 963-975.
[11] Basta G, Schmidt AM and De Caterina R. Advanced glycation end products and vascular inflammation: implications for accelerated atherosclerosis in diabetes. Cardiovasc Res 2004; 63: 582-592.
[12] Semba RD, Bandinelli S, Sun K, Guralnik JM and Ferrucci L. Plasma carboxymethyl-lysine, an advanced glycation end product, and all-cause and cardiovascular disease mortality in older community-dwelling adults. J Am Geriatr Soc 2009; 57: 1874-1880.
[13] Liu J, Masurekar MR, Vatner DE, Jyothirmayi GN, Regan TJ, Vatner SF, Meggs LG and Malhotra A. Glycation end-product cross-link breaker reduces collagen and improves cardiac function in aging diabetic heart. Am J Physiol Heart Circ Physiol 2003; 285: H2587-2591.
[14] Ambros V. The functions of animal microRNAs. Nature 2004; 431: 350-355.
[15] Bartel DP. MicroRNAs: genomics, biogenesis, mechanism, and function. Cell 2004; 116: 281-297.
[16] van Rooij E and Olson EN. MicroRNAs: powerful new regulators of heart disease and provocative therapeutic targets. J Clin Invest 2007; 117: 2369-2376.
[17] Hamburg NM and Leeper NJ. Therapeutic potential of modulating microRNA in peripheral artery disease. Curr Vasc Pharmacol 2015; 13: 316-323.
[18] Saugstad JA. MicroRNAs as effectors of brain function with roles in ischemia and injury, neuroprotection, and neurodegeneration. J Cereb Blood Flow Metab 2010; 30: 1564-1576.
[19] Neale JP, Pearson JT, Katare R and Schwenke DO. Ghrelin, microRNAs, and critical limb ischemia: hungering for a novel treatment option. Front Endocrinol (Lausanne) 2017; 8: 350.
[20] Roberts DD. Thrombospondins: from structure to therapeutics. Cell Mol Life Sci 2008; 65: 669-671.
[21] Wang JM, Tao J, Chen DD, Cai JJ, Irani K, Wang Q, Yuan H and Chen AF. MicroRNA miR-27b rescues bone marrow-derived angiogenic cell function and accelerates wound healing in type 2 diabetes mellitus. Arterioscler Thromb Vasc Biol 2014; 34: 99-109.
[22] Miao X, Rahman MF, Jiang L, Min Y, Tan S, Xie H, Lee L, Wang M, Malmstrom RE, Lui WO and Li N. Thrombin-reduced miR-27b attenuates platelet angiogenic activities in vitro via enhancing platelet synthesis of anti-angiogenic thrombospondin-1. J Thromb Haemost 2018; 16: 791-801.
[23] You J, Sun J, Ma T, Yang Z, Wang X, Zhang Z, Li J, Wang L, Ii M, Yang J and Shen Z. Curcumin induces therapeutic angiogenesis in a diabetic mouse hindlimb ischemia model via modulating the function of endothelial progenitor cells. Stem Cell Res Ther 2017; 8: 182.
[24] Wang C, Yue F and Kuang S. Muscle histology characterization using H&E staining and muscle fiber type classification using immunofluorescence staining. Bio Protoc 2017; 7.
[25] Xin B, He X, Wang J, Cai J, Wei W, Zhang T and Shen X. Nerve growth factor regulates CD133 function to promote tumor cell migration and invasion via activating ERK1/2 signaling in pancreatic cancer. Pancreatology 2016; 16: 1005-1014.
[26] Hamada H, Kim MK, Iwakura A, Ii M, Thorne T, Qin G, Asai J, Tsutsumi Y, Sekiguchi H, Silver M, Wecker A, Bord E, Zhu Y, Kishore R and Losordo DW. Estrogen receptors alpha and beta me-

diate contribution of bone marrow-derived endothelial progenitor cells to functional recovery after myocardial infarction. Circulation 2006; 114: 2261-2270.
[27] Nehler MR, Duval S, Diao L, Annex BH, Hiatt WR, Rogers K, Zakharyan A and Hirsch AT. Epidemiology of peripheral arterial disease and critical limb ischemia in an insured national population. J Vasc Surg 2014; 60: 686-695, e682.
[28] Norgren L, Hiatt WR, Dormandy JA, Nehler MR, Harris KA, Fowkes FG, Bell K, Caporusso J, Durand-Zaleski I, Komori K, Lammer J, Liapis C, Novo S, Razavi M, Robbs J, Schaper N, Shigematsu H, Sapoval M, White C, White J, Clement D, Creager M, Jaff M, Mohler E 3rd, Rutherford RB, Sheehan P, Sillesen H and Rosenfield K. Inter-society consensus for the management of peripheral arterial disease (TASC II). Eur J Vasc Endovasc Surg 2007; 33 Suppl 1: S1-75.
[29] Yla-Herttuala S, Bridges C, Katz MG and Korpisalo P. Angiogenic gene therapy in cardiovascular diseases: dream or vision? Eur Heart J 2017; 38: 1365-1371.
[30] Effect of intensive blood-glucose control with metformin on complications in overweight patients with type 2 diabetes (UKPDS 34). UK Prospective Diabetes Study (UKPDS) Group. Lancet 1998; 352: 854-865.
[31] Brownlee M. Biochemistry and molecular cell biology of diabetic complications. Nature 2001; 414: 813-820.
[32] Watson AM, Gray SP, Jiaze L, Soro-Paavonen A, Wong B, Cooper ME, Bierhaus A, Pickering R, Tikellis C, Tsorotes D, Thomas MC and Jandeleit-Dahm KA. Alagebrium reduces glomerular fibrogenesis and inflammation beyond preventing RAGE activation in diabetic apolipoprotein E knockout mice. Diabetes 2012; 61: 2105-2113.
[33] Vaitkevicius PV, Lane M, Spurgeon H, Ingram DK, Roth GS, Egan JJ, Vasan S, Wagle DR, Ulrich P, Brines M, Wuerth JP, Cerami A and Lakatta EG. A cross-link breaker has sustained effects on arterial and ventricular properties in older rhesus monkeys. Proc Natl Acad Sci U S A 2001; 98: 1171-1175.
[34] Bitto A, Minutoli L, Galeano MR, Altavilla D, Polito F, Fiumara T, Calo M, Lo Cascio P, Zentilin L, Giacca M and Squadrito F. Angiopoietin-1 gene transfer improves impaired wound healing in genetically diabetic mice without increasing VEGF expression. Clin Sci (Lond) 2008; 114: 707-718.
[35] Good DJ, Polverini PJ, Rastinejad F, Le Beau MM, Lemons RS, Frazier WA and Bouck NP. A tumor suppressor-dependent inhibitor of angiogenesis is immunologically and functionally indistinguishable from a fragment of thrombospondin. Proc Natl Acad Sci U S A 1990; 87: 6624-6628.
[36] Bhattacharyya S, Marinic TE, Krukovets I, Hoppe G and Stenina OI. Cell type-specific post-transcriptional regulation of production of the potent antiangiogenic and proatherogenic protein thrombospondin-1 by high glucose. J Biol Chem 2008; 283: 5699-5707.
[37] Dubois S, Madec AM, Mesnier A, Armanet M, Chikh K, Berney T and Thivolet C. Glucose inhibits angiogenesis of isolated human pancreatic islets. J Mol Endocrinol 2010; 45: 99-105.
[38] Bazzazi H, Zhang Y, Jafarnejad M, Isenberg JS, Annex BH and Popel AS. Computer simulation of TSP1 inhibition of VEGF-Akt-eNOS: an angiogenesis triple threat. Front Physiol 2018; 9: 644.
[39] Calin GA and Croce CM. MicroRNA-cancer connection: the beginning of a new tale. Cancer Res 2006; 66: 7390-7394.
[40] Feinberg MW and Moore KJ. MicroRNA regulation of atherosclerosis. Circ Res 2016; 118: 703-720.
[41] Biyashev D, Veliceasa D, Topczewski J, Topczewska JM, Mizgirev I, Vinokour E, Reddi AL, Licht JD, Revskoy SY and Volpert OV. miR-27b controls venous specification and tip cell fate. Blood 2012; 119: 2679-2687.
[42] Zhu J, Yang K, Jing Y, Du R, Zhu Z, Lu L and Zhang R. The effects of low-dose nepsilon-(carboxymethyl) lysine (CML) and nepsilon-(carboxyethyl) lysine (CEL), two main glycation free adducts considered as potential uremic toxins, on endothelial progenitor cell function. Cardiovasc Diabetol 2012; 11: 90.
[43] Duranton F, Cohen G, De Smet R, Rodriguez M, Jankowski J, Vanholder R and Argiles A. Normal and pathologic concentrations of uremic toxins. J Am Soc Nephrol 2012; 23: 1258-1270.

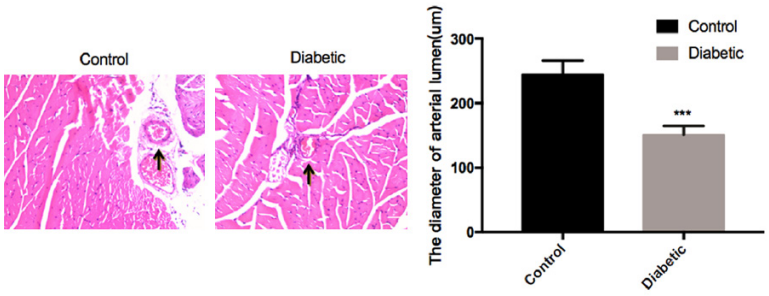

Supplementary Figure 1. Angiogenesis repair was impaired in the ischemic hindlimbs of diabetic mice. The diameter of the intermuscular artery lumen in ischemic hindlimbs of diabetic mice was decreased comparing with that in normal mice, suggesting the suppressed blood flow performed in diabetic mice. Representative images are presented on the left and the quantitative analysis was performed using Image J. (Scale bar = 200 μm; n = 8 per group; $^{***}P < 0.001$).

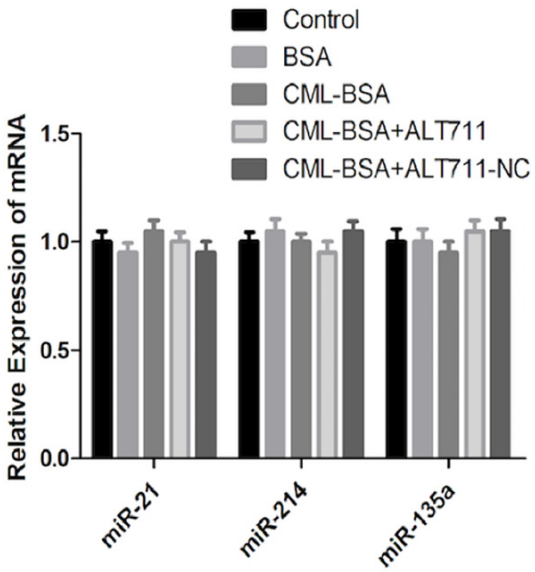

Supplementary Figure 2. MiRNA expression of HUVECs in CML-BSA and HUVECs treated with ALT-711 in CML-BSA. There was no outstanding difference in miR-21, miR-214, and miR-135a expression between the groups. ($P > 0.05$, n = 3).